Low Level RF and Timing for IOTA ring

- Summer Student Program at Fermi National Accelerator Laboratory -

Final Report

September 28, 2018

Author:
Francesco Bruni

Supervisors:
Kermit Carlson
Dean Edstrom
Alexander Valishev

APC IOTA/FAST Department
NML Building
Fermilab
https://fast.fnal.gov/

Title:
Low Level RF and Timing for IOTA ring

Subjects:
RF electronics, Accelerator technology, RF cavities, PLC programming

Project Period:
August and September 2018

Research Group:
FAST, Accelerator Division

Supervisors:
Kermit Carlson
Dean Edstrom
Alexander Valishev

Date of Completion:
September 28, 2018

Abstract:

The Project I carried out consisted in the assembly and characterization of the low-level RF controller for the electron RF cavity of IOTA.
IOTA is the storage ring of a new particle accelerator at Fermilab, completed in august 2018 and under commissioning at present. It is intended to work both with electrons and protons, and to be used to conduct experiments about accelerator technology.
In this report I will present briefly the structure of the accelerator, then describe the low-level RF system, its assembly phase and its first simple characterizations. I will proceed with the installation in site, software programming and calibration of the sensitive components. In conclusion, the last chapter describes the repair of the RF cavity after a severe damage.

Operated by Fermi Research Alliance, LLC under Contract No. DE-AC02-07CH11359 with the United States Department of Energy.

Contents

Chapter 1

Introduction

Fermilab Accelerator Science and Technology (FAST) facility is a section of the Accelerator Division at Fermilab with the mission to develop a fully-equipped R&D accelerator chain to support research about accelerator technology. The aim of the structure is to study the limitations to beam intensity, to develop new approaches to particle-beam generation, acceleration and manipulation, and to test SRF accelerators and high brightness beam applications; in one phrase to explore the future of accelerator technology. The acceleration construction was completed the first days of august 2018, so the first beam experiments are being carried out at present.

The main components of FAST facility are a linear accelerator and a storage ring (namely IOTA, Integrable Optics Test Accelerator).

1.1 Linear Accelerator

The heart of the linac is a RF photoinjector (scheme in Figure 1.1), whose electron source is a 1-1/2 cell RF-gun with a Cs_2Te photocathode. The photocathode is excited by an UV laser source modulated in trains of bunches repeated at 3 MHz within 1-ms-duration macropulse (the waveform of the laser source is represented in Figure 1.2). The 5-MeV electrons coming from the RF-gun are accelerated with a couple of superconducting RF cavities to 50 MeV, and then focused with a set of quadrupole magnets. Some steering dipole magnets form a four-bend magnetic compression chicane, with the purpose to compress the electrons bunch longitudinally while preserving the beam's transverse emittance.

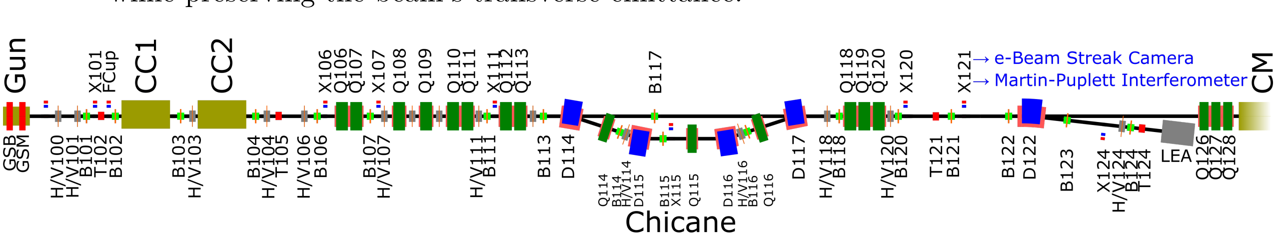

Figure 1.1: Scheme of the linear accelerator section

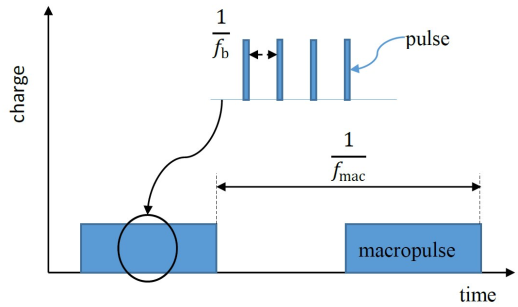

Figure 1.2: Waveform of the laser source: $f_b = 30\,\text{MHz}$, $fmac \approx \text{Hz}$, $T_{macropulse} = 1\,\text{ms}$

After the chicane, some dipoles allow to steer the beam inside a low-energy absorber, or let it pass through to the accelerating stages, composed of 1.3 GHz SRF Cryomodules. The beam can then go straight into a high-energy absorber or can be bent with a Lambertson magnet to enter the IOTA storage ring.

The Superconducting RF cryomodules can accelerate the electron beam up to 300 MeV, placing the nominal IOTA injection energy of 150 MeV well within this range. Note that there is space available in the existing beamline that would allow for additional cryomodules to bring the total beam energy to ∼1.5 GeV in the future.

1.2 IOTA Ring

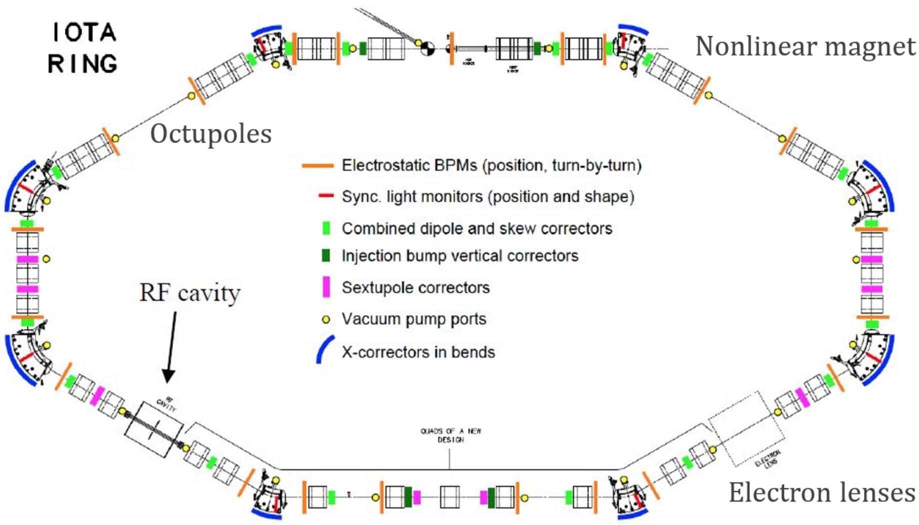

Figure 1.3: Scheme of the IOTA ring

IOTA is a small (39 meters long) storage ring, whose main research topics include the possibility of using integrable optics with nonlinear magnets and electron lenses, techniques for space-charge compensation and optical stochastic cooling. It is intended to be used both with protons and electrons, and for this reason a proton injector will be added in the future. In particular, the energies of particles intended to circulate is 150 MeV for electrons and 2.5 MeV for protons.

The IOTA ring is composed of 8 straight sections, separated by 8 dipole magnets, as shown schematically in Figure 1.3. A lot of quadrupole and sextupole magnets are used along the ring for dispersion suppression and chromaticity correction. The top horizontal section is used for the beam injection (one Lambertson magnet and a couple of electromagnetic stripline kickers), while the lower-left diagonal section is reserved for an accelerating RF cavity. The other long sections can be used for the installation of experimental apparatus, such as octupoles, nonlinear magnets and electron lenses.

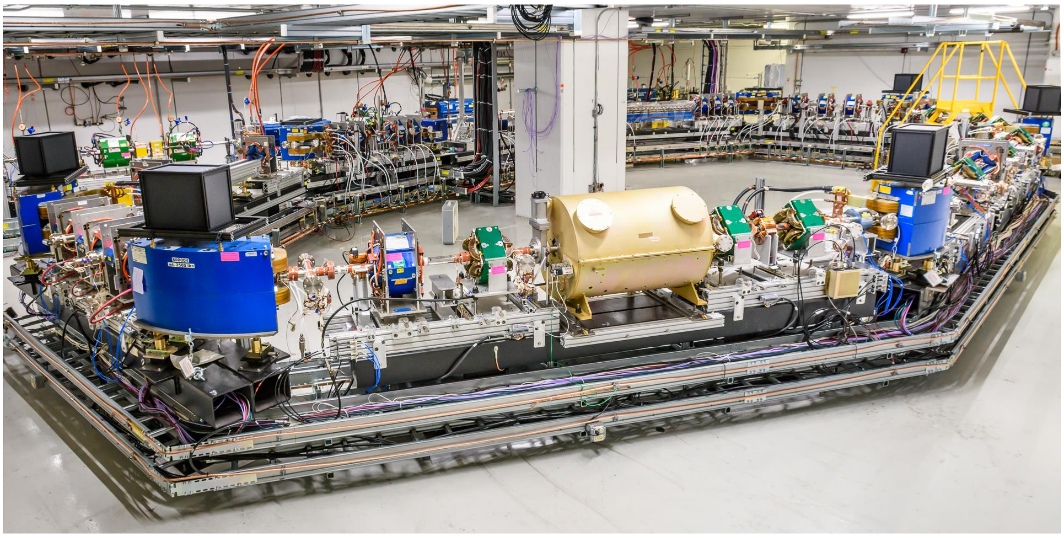

Figure 1.4: Photo of the IOTA ring, the RF cavity is the golden cylindrical structure in the foreground

Chapter 2

Overview of the RF System

The project carried out was focused on the low-level RF system of the IOTA ring, whose main component is the RF cavity. The RF cavity is the component needed to "bunch" the beam, i.e. to create packets of particles running inside the accelerator instead of having a continuous ("DC") beam. Bunching of the beam is important because it allows to use the Beam Position Monitors (BPMs) to measure the position of particles throughout their motion inside the accelerator. The BPMs in fact do not work properly with unbunched beams. The RF cavity is also essential as it provides the particles with some acceleration to compensate for the synchrotron losses. Without this energy replenishment particles would progressively lose momentum, spiral down and eventually get lost after a few thousands turns.

2.1 The RF Cavity

The RF cavity is a dual-frequency system: it is composed of two separate cavities operating at 30 MHz and 2.18 MHz. Calculations show that these frequencies correspond to the fourth revolution harmonic for a 150 MeV electron beam and a 2.5 MeV proton beam, respectively. This means that the frequency of the RF wave is 4 times higher than that of revolution of particles inside the accelerator, and therefore the ring can contain up to 4 spatially-separated bunches at a time, but for normal operative conditions it was decided that only one bunch will be occupied by particles.

When the electron beam is present only the 30 MHz section of the cavity is excited, while with protons both frequencies are used: the 2.18 MHz signal provides the bunching at the fourth harmonic, while the 30 MHz wave modulates the proton bunch making it observable with the BPMs. The BPMs, in fact, work properly only at 30 MHz.

A section view of the cavity is shown in Figure 2.1. It consists of a cylindrical aluminum frame hosting the pipe and a big disk separator with good electrical contacts to shield the 30 MHz section from the 2.18 MHz one. The pipe is loaded with ferrite disks in order to increase the equivalent inductance of the system and be able to reach a quality factor Q for the oscillations in the order of 100. At the entrance of the cavity the aluminum pipe is interrupted with a 2-inch long ceramic break: this introduces a capacitance between the aluminum pipe inside the cavity and the ground potential, allowing to apply the high-voltage, high power signals directly to the pipe itself.

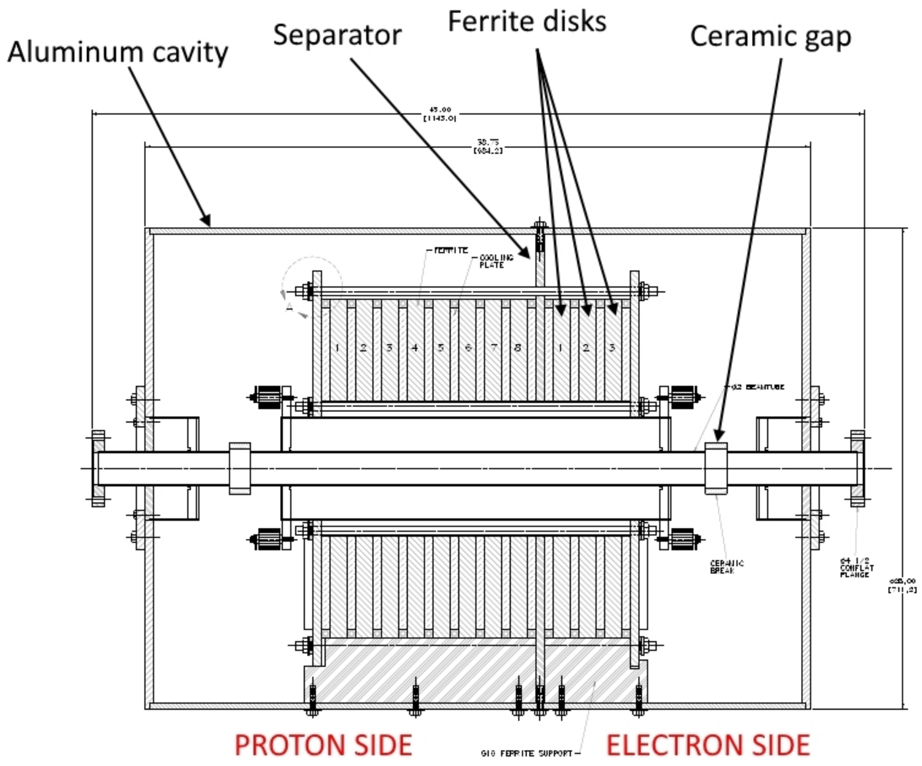

Figure 2.1: Section view of the RF accelerating cavity

2.2 Phase and Amplitude Controller for Electrons

Figure 2.2 shows a scheme of the RF low-level subsystem for the bunching of electrons. A 30 MHz oscillator is used as a reference source and is fed inside a directional coupler (DC), which spills a reduced amount of power from the oscillation as a reference signal for the timing section. The DC is followed by a variable phase shifter (model JSPHS-51+) and a voltage variable attenuator (model ZX73-2500+), both controlled by 0÷10 V signals coming from a Programmable Logic Controller (PLC). The phase shifter introduces a delay to synchronize the RF oscillation with the revolution of the particle bunch, while the attenuator adjusts the power fed to the cavity. The signal is now in the 10 dBm range, and is processed by a solid-state power amplifier (PA) with a maximum output power of approximately 200 W. A relay switch is used as a safety switch: when the relay is powered the oscillation gets transmitted to the power amplifier, otherwise the input of the PA is connected to a 50 Ω termination. This termination not only breaks the signal chain, but also prevents any noise from being amplified when the switch is off.

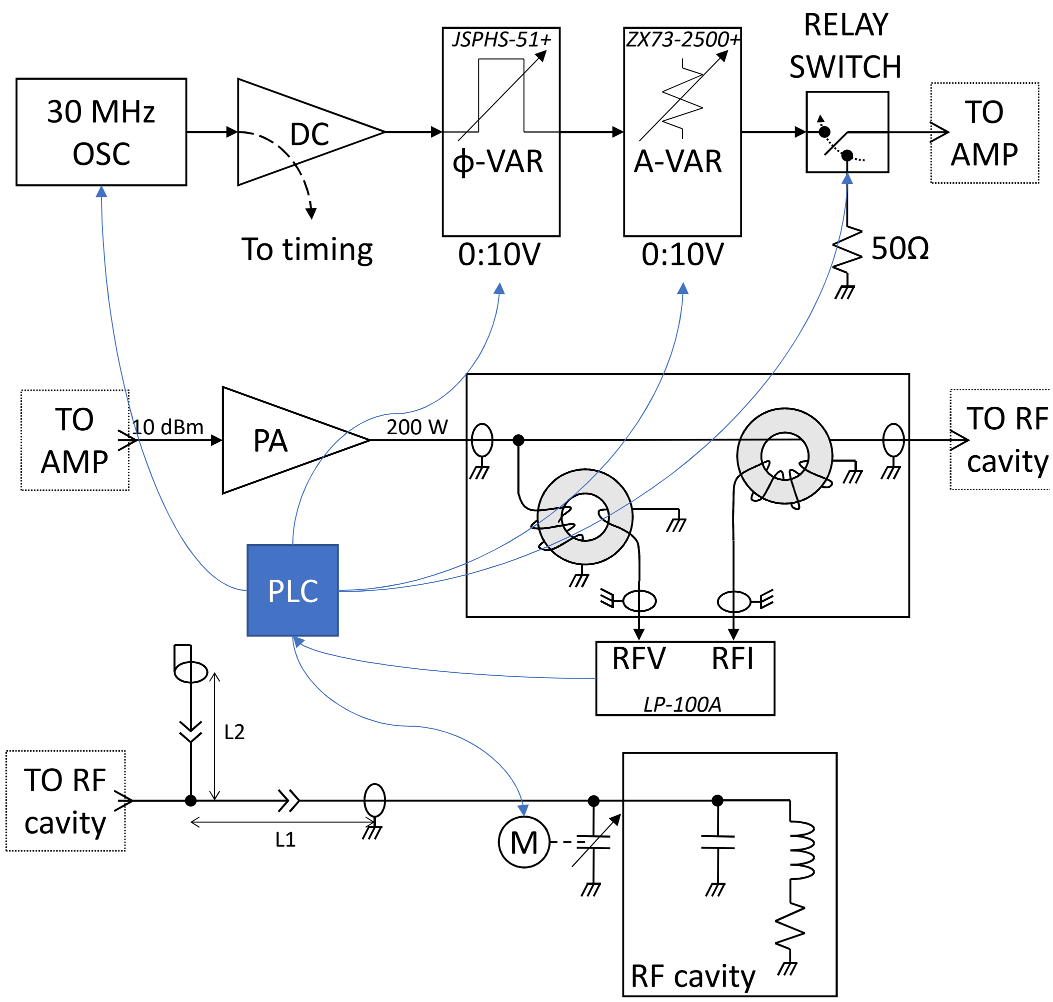

Figure 2.2: Scheme of the low level RF system for the bunching of electrons

The power signal then passes through a directional coupler, which uses two toroidal transformers to pick up the signals corresponding to the voltage and current supplied to the load. These signals are fed into a Digital Vector RF Wattmeter (model LP-100A) to measure the relative phase between current and voltage, which represents the quality of the impedance matching obtained inside the cavity. The RF cavity in fact is driven in resonance conditions, which means that an impedance matching network is used to assure that the RF power is transmitted with the maximum efficiency possible and without reflections. The electrical model of the cavity is analogous to the parallel of a capacitor and a R-L series; to obtain the

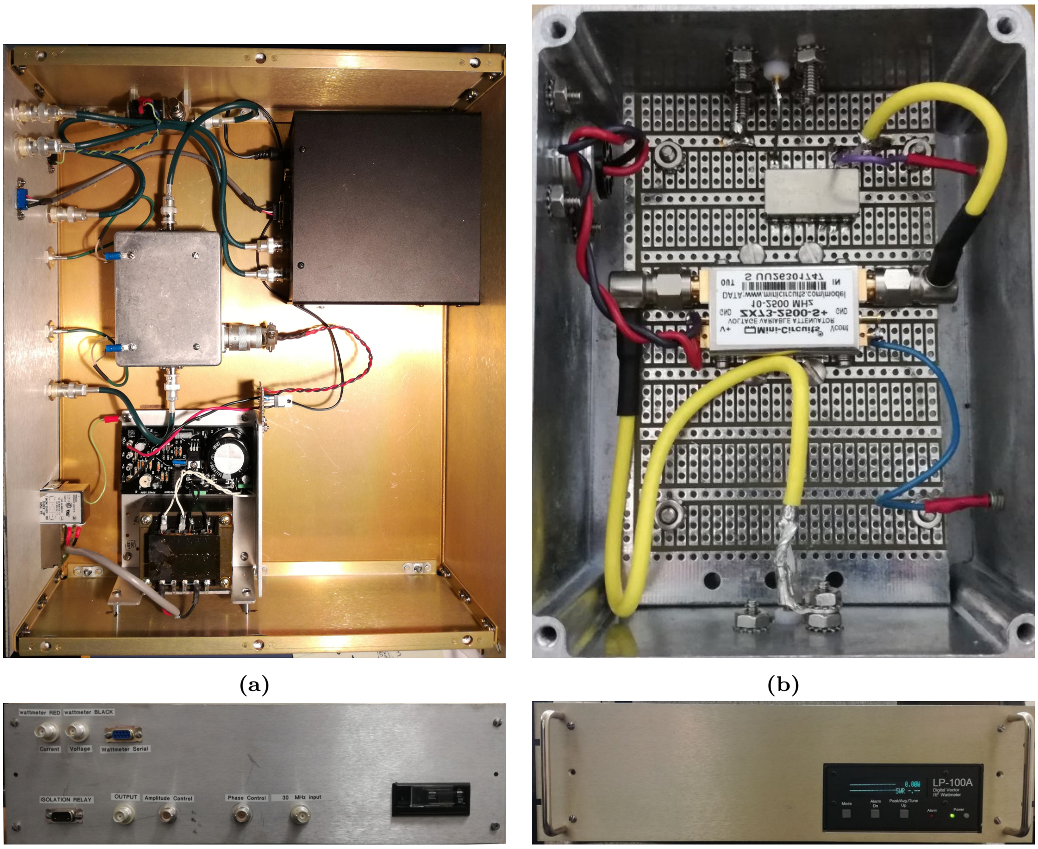

(a) (b) (c) (d)

Figure 2.3: Photos of the phase and amplitude controller system: **(a)** A view inside the phase and amplitude controller system. From the top right corner, the black box is the LP-100A vector RF wattmeter, the metallic box contains the variable phase shifter and variable attenuator, and the exposed transformer and electronic board are a 12V DC power supply. **(b)** Photo of the variable phase shifter and variable attenuator box. **(c)** A view of the back of the system, with labeled connectors. **(d)** Photo of the front of the system, with a window for the wattmeter.

impedance matching a parallel stub network is used, where the stub is made of a short section of transmission line closed in short circuit (L2). In order to allow fine tuning of the resonance conditions (for example against temperature fluctuations, power variations, etc.) a variable capacitor is mounted in parallel to the feeding line, and driven by a stepper motor.

The photos in Figure 2.3 show the phase and amplitude controller system, containing some of the components of the previous diagram.

2.3 Phase and Amplitude Controller Characterizations

After the building of the phase and amplitude controller subsystem, some characterizations of the system have been made. The main instruments used for these measurements are: a RF signal generator, a RF wattmeter, a DC voltage generator and a digital oscilloscope.

First of all, the behavior of the variable attenuator has been studied, and for this purpose the system has been fed in input with a 30 MHz oscillation, and the power of the output oscillation has been measured. By varying the power of the input oscillation and the DC voltage supplied to the variable attenuator, it has been possible to obtain the characteristics shown in Figure 2.4.

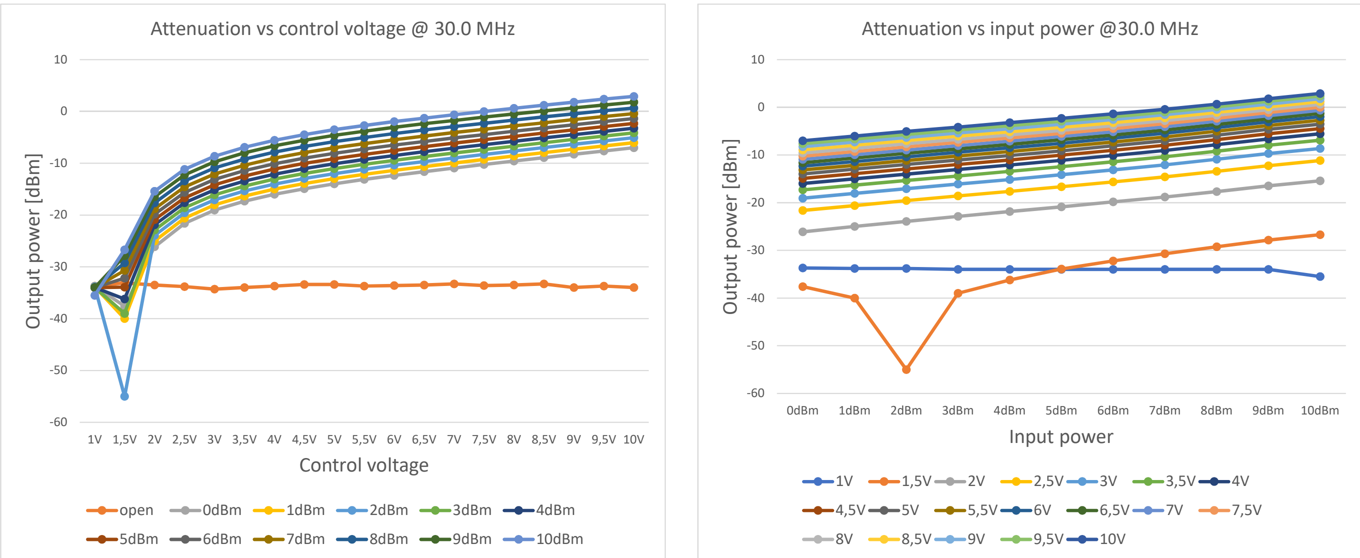

(a) (b)

Figure 2.4: **(a)** Output power vs control voltage on the variable attenuator, for different values of the input power, as shown in the legend. **(b)** Output power vs input power, for different values of the control voltage on the variable attenuator, as shown in the legend.

It can be noted that some curves deviate from the behavior of the others: first of all the orange points of Figure 2.4(a). As indicated by the legend, these points correspond to the case when the input is left open, so no 30 MHz wave is present and the output corresponds to the noise level of the system and instrumentation. Also in Figure 2.4(b) two curves have an anomalous behavior: the blue and the orange one, relative to the lowest control voltages. The reason is that they correspond to the highest attenuation possible, so the output power appears to be lower than or comparable to the just discussed noise level, and this affects the quality of the measurement.

It is interesting to observe the ranges of linearity for the attenuator. While the attenuation is fairly linear across the range of input powers for various fixed control voltages as shown in Figure 2.4(b), in practice the control voltage is adjusted. This drops off steeply below 3 V, as shown in 2.4(a), and the spread of the curves in both characterizations indicated that calibration would be required after final installation.

Also the phase delay was put under test, and the results are shown in Figure 2.5, from which it is possible to observe that the linear range for the relative phase shift is approximately between 0° and 90°.

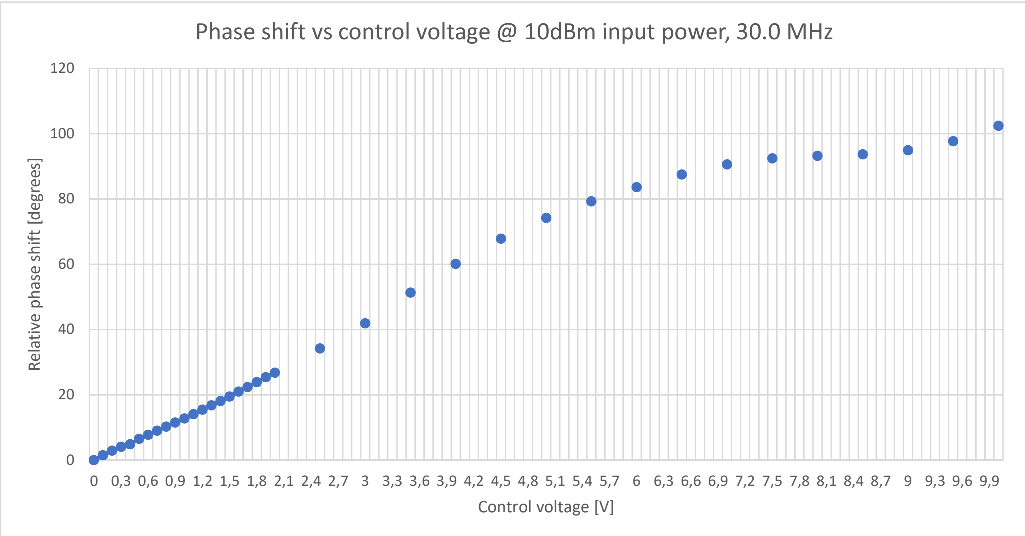

Figure 2.5: Phase delay introduced by the system vs control voltage

Chapter 3

Software Development

3.1 PLC Side Programming

After the above described characterization, the phase and amplitude controller system was connected to the 30 MHz oscillator, the power amplifier and the PLC. It was then necessary to program the PLC in order to install this new system.

The PLC (namely Programmable Logic Controller) is an industrial computer frequently used for automation control because it is reliable, relatively powerful in terms of computation, easy to build and to connect to external hardware. It can also be relatively inexpensive compared to some other controls solutions. The model used is the Productivity2000 from AutomationDirect, already present in the lab and connected to other subsystems. The PLC modules installed are shown in Figure 3.1 and are the following (from left to right):

- 24 V DC power supply
- CPU module, model P2-550: 32-bit CPU with Ethernet connection, one RS-232 port and one RS-485
- digital to analog converter module: 8 channels, 16 bit resolution and $-10\,\mathrm{V} \div 10\,\mathrm{V}$ output range
- analog to digital converter module: 8 channels, 16 bit resolution and $0\,\mathrm{V} \div 10\,\mathrm{V}$ input range
- digital output module: 16 pin
- digital input module: 16 pin
- serial communications module: three RS-232 ports and one RS-485

The PLC was already programmed for the connection with the LP-100A wattmeter (using the COM0 serial port of the CPU module), so the only section developed was the control of phase and amplitude of the oscillation. The PLC is connected to

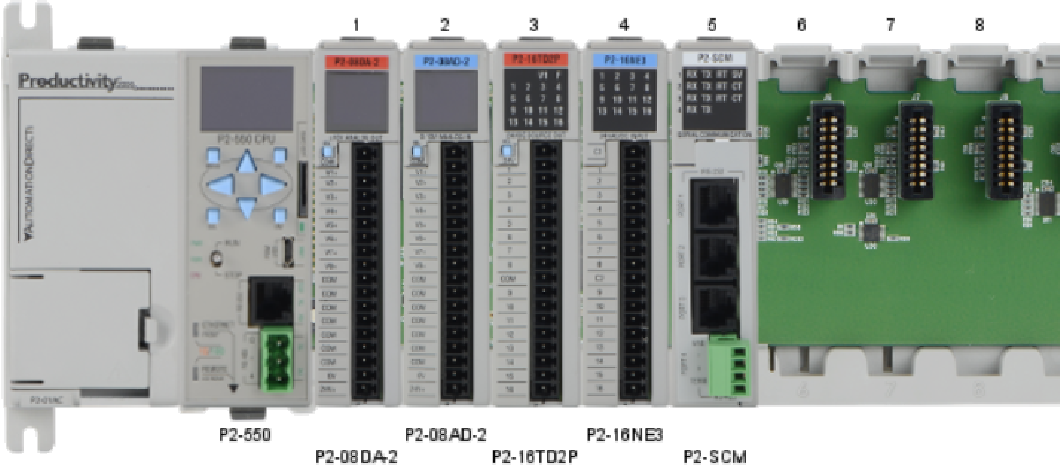

Figure 3.1: PLC modules installed

the Fermilab ACNET (Accelerator Controls NETwork), a database from which it receives the commands and set-points, and to which it provides feedbacks about the actuations. The problem was therefore to develop a PLC software able to acquire from ACNET the desired phase shift and attenuation, to properly generate the necessary control voltages and to inform ACNET of the correct driving of the system.

It was decided to use two outputs from the DAC module to generate the control voltages for the phase shifter and attenuator, while as regards the connection to ACNET it was already implemented via Ethernet. One channel from the digital output module was then used to generate the control signal for the relay switch.

The PLC is programmed using *ladder logic*, a graphical programming language based on the style of the relay logic. The instructions are represented with blocks on horizontal rungs, and are executed sequentially, from left to right inside each rung and from the top rung to the bottom rung.

The simple algorithm developed for phase and amplitude control is shown in the form of ladder logic in Figure 3.2. Since the software is pretty simple, each rung has only one instruction and no branches, so the system at each iteration will simply execute all of the instructions in sequence, from the top rung to the bottom one.

The first four instructions are related to phase control:

1. The desired phase shift is acquired as an input from ACNET (*myPCe_AI* stands for 'my Phase Control for electrons, Input from ACNET') and a transformation function is applied to obtain the necessary control voltage. The transformation function between phase shift and control voltage (and vice versa) derives from a fitting of experimental data, and will be explained later in this document.

   This control voltage is then converted in counts for the DAC output. The out-

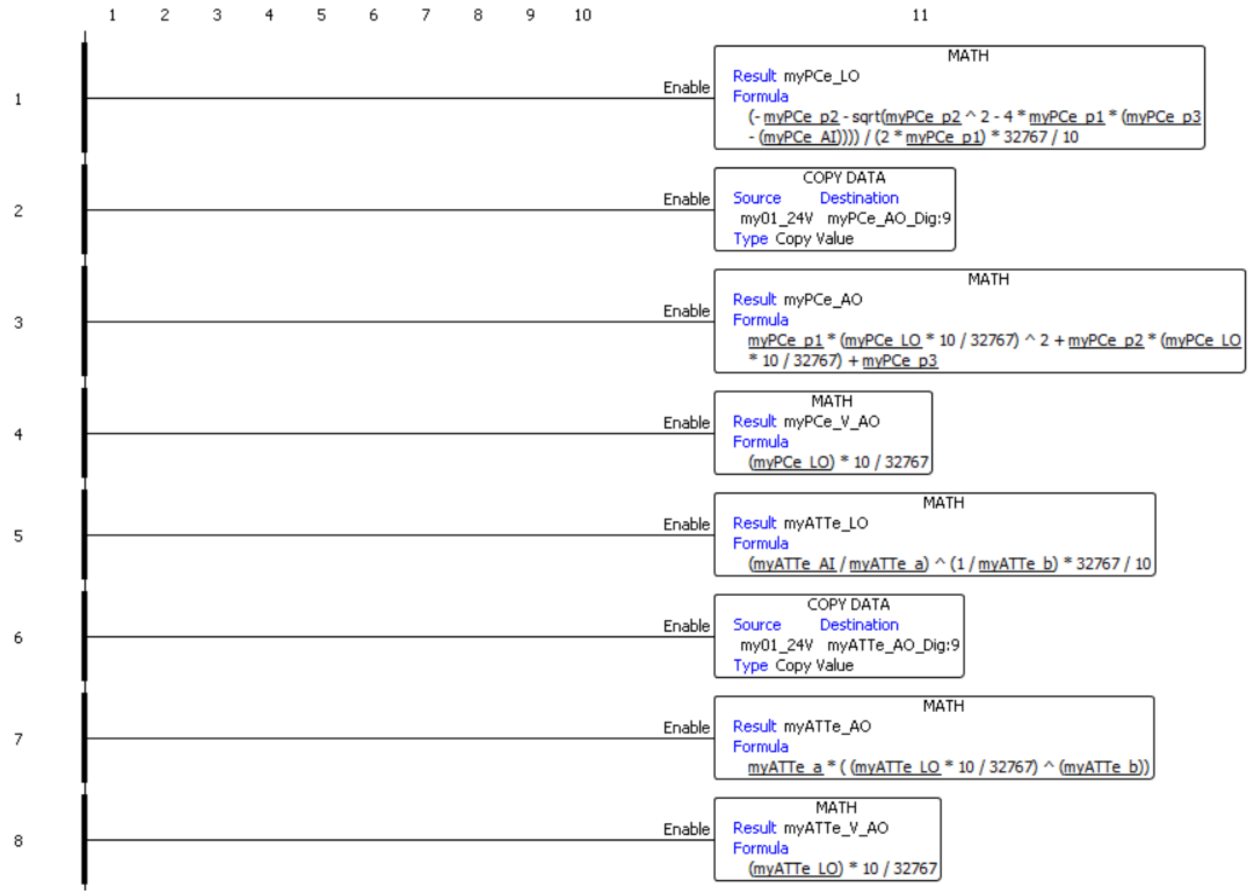

Figure 3.2: Ladder logic program for the PLC phase and amplitude control

put voltage range $-10\,\mathrm{V} \div 10\,\mathrm{V}$ is linearly mapped in the counts range -32768 $\div$ +32767. The desired voltage therefore needs to be multiplied by 32767/10 to obtain the number of counts.

2. The signal indicating the presence of the 24V supply to the DAC module (*my01_24V*) is sent to ACNET for fault detection purposes.

3. The inverse of the transformation function is applied to the DAC counts and the obtained phase shift is sent as an output to ACNET (*myPCe_AO*).

4. The raw output voltage, as obtained from the number of counts, is sent to ACNET for read-back purposes (*myPCe_V_AO*).

The other four rungs are relative to the attenuator control, and their instructions are analogous to the previous ones.

Table 3.1 shows a synthesis of the connections between the PLC and the phase and attenuation control system, and for each connection the name of the relative variable in the PLC software is shown.

Slot	Port	PLC variable name	Connected to
0 - CPU Module (P2-550)	RS-232	myCom0	LP-100A Wattmeter serial
1 - DAC Module (P2-08DA-2)	Channel 3	myPCe_LO	Phase shifter control voltage
1 - DAC Module (P2-08DA-2)	Channel 4	myATTe_LO	Attenuator control voltage
3 - Digital output Module (P2-16TD2P)	Channel 1	myRFEnab_LO	Isolation relay

Table 3.1: PLC connections and relative variables

3.2 ACNET Side Programming

For the interface and control of the PLC it was necessary to create four devices on the ACNET network: two for the phase control and two for the attenuation control. An ACNET device is a software entity whose functions are (among others):

- To **READ** the content of a memory area containing float values: this function was used to retreive the "Output to ACNET" ($\_AO$) variables from the PLC
- To **SET** the content of a memory area containing float values: this function was used to set the "Input from ACNET" ($\_AI$) variables in the PLC
- To **CONTROL** the digital status of the system
- To read the digital **STATUS** of the system: this function was used to acquire data for fault detection, i.e. to retrieve the "Output to ACNET Digital" ($\_AO\_Dig$) variables from the PLC

Each of these functions is associated inside ACNET to a SSDN code, a 16-digit hexadecimal word with the following structure:

$$< aabb/00d0/00ee/02cc >$$

where each letter stands for:

- aa is the attribute, i.e. the type of performed I/O. $aa = 03$ stands for 16-bit Integer register read, $aa = 04$ for 16-bit Integer register write and $aa = 06$ for 32-bit float register read/write.
- bb is the ID number of the PLC, to identify it since more than one PLC is connected to ACNET. In the case of IOTA RF PLC, $bb = 19$.
- cc is the so-called Erlang Modbus address. Not all of the variables inside the PLC can be accessed by ACNET, but only the ones connected to the Modbus. When a variable is added to the Modbus it receives an address that identifies it on the bus itself.

ACNET device name	Description	Reading		Setting		Status	
		PLC Variable	**Addr**	**PLC Variable**	**Addr**	**PLC Variable**	**Addr**
N:IRFEPC	Phase Control	*myPCe_AO*	0x45	*myPCe_AI*	0x42	*myPCe_AO_Dig*	0x44
N:IRFEAT	Attenuation Control	*myATTe_AO*	0x4B	*myATTe_AI*	0x47	*myATTe_AO_Dig*	0x49
N:IRFEAV	Attenuation Control V	*myATTe_V_AO*	0x4F				
N:IRFEPV	Phase Control V	*myPCe_V_AO*	0x4D				

Table 3.2: ACNET devices created for the phase and amplitude controller system. For each device the names and the Modbus addresses of the relative variables inside the PLC are shown. The column relative to the control function has been omitted because it wasn't used by any of the devices created.

- d is for Read Only/Write (respectively 0/1)
- ee is the address for the reflected write. It is used only in write mode, and indicates where to read-back the result of a write operation. For normal operation $ee = cc$, which means the read-back is made on the same register that is being written.

As an example, for the reading of the 32-bit float register *myPCe_AO*, with a Modbus address = 70 (dec) the SSND is:

$$< 0619/0000/0000/0245 >$$

Note that 70 (dec) corresponds to 46 (hex), but the SSDN contains $cc = 45$ because the first address is 1 for the PLC and 0 for ACNET.

Table 3.2 shows the ACNET devices created for the phase and amplitude controller system, and the relative variables names inside the PLC and Modbus addresses.

3.2.1 Attenuation Calibration

The data obtained in Section 2.3 and shown in Figure 2.4 proved to be accurate once the system was connected to the power amplifier. However, to take into account the behaviour of the whole system, it was decided to perform a new set of measurements. A 50 Ω load was connected to the output of the LP-100 directional coupler (for reference see Figure 2.2) and the signals RFV and RFI were used through the LP-100A wattmeter to measure the power fed to the load for different attenuation control voltages. One other wattmeter (model HP 437B) was connected to the output of the load and was used to measure the power fed to the load and attenuated by the load itself of a factor of 30 dB. This double measurement was necessary to evaluate the linearity of the response of the LP-100A wattmeter.

In this measurement the only part of the system not present was the real RF cavity with its impedance matching network, substituted by the dummy load. As a difference from what measured in Section 2.3, therefore, also the behaviour of the power amplifier and of the connection cables was now taken into account.

The data acquisition was carried out with an automated procedure, since the system was already connected and controllable through ACNET. A simple ACL (Accelerator Control Language) script for setting the attenuation control voltage and reading the output of the LP-100A wattmeter was written, and can be found in the Appendix A.

Also the HP 437B wattmeter was accessible via software, with the *telnet* protocol, and for the reading of its output a python script was written, and is shown in appendix A. To match the data measured by the two wattmeters, a timestamp was registered and associated to each measured value.

The acquired points were then translated accordingly to the information provided by the first characterization (section 2.3), in order to obtain the attenuation. The measured attenuation points are represented in blue and green in Figure 3.3.

From these data, a fitting function was derived using a power function and the least squares method on Matlab. The result of this operation is the red curve of Figure 3.3.

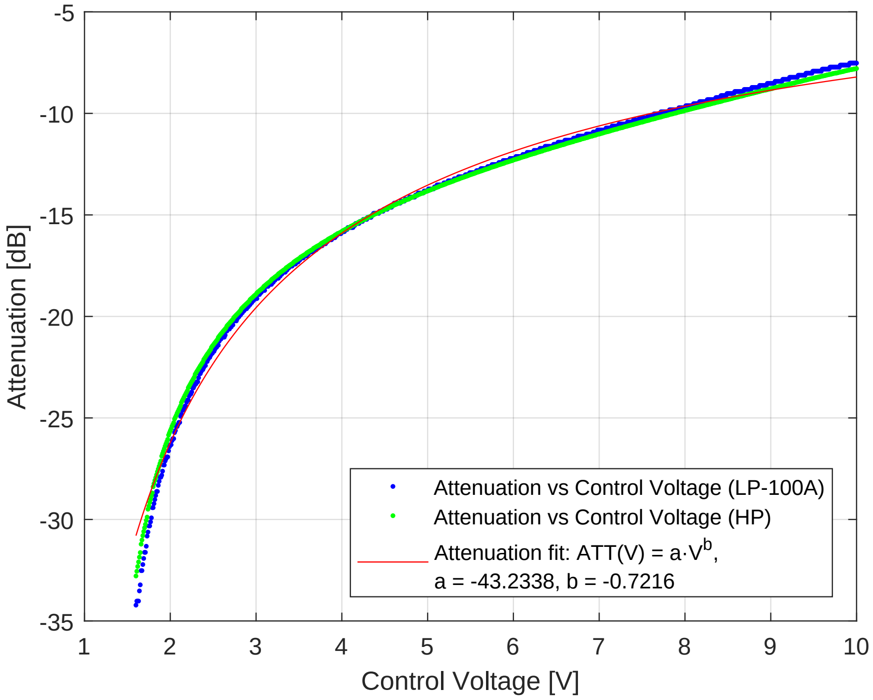

Figure 3.3: Results of the attenuation calibration fitting

3.2.2 Phase Shift Calibration

A new set of measurements was performed also for the variable phase shifter: an oscilloscope was connected both to the 30MHz reference wave produced by the oscillator and to the output of the 50 Ω load fed by the power amplifier. This allowed to measure the relative phase between the two waves, as shown in the photo of Figure 3.4.

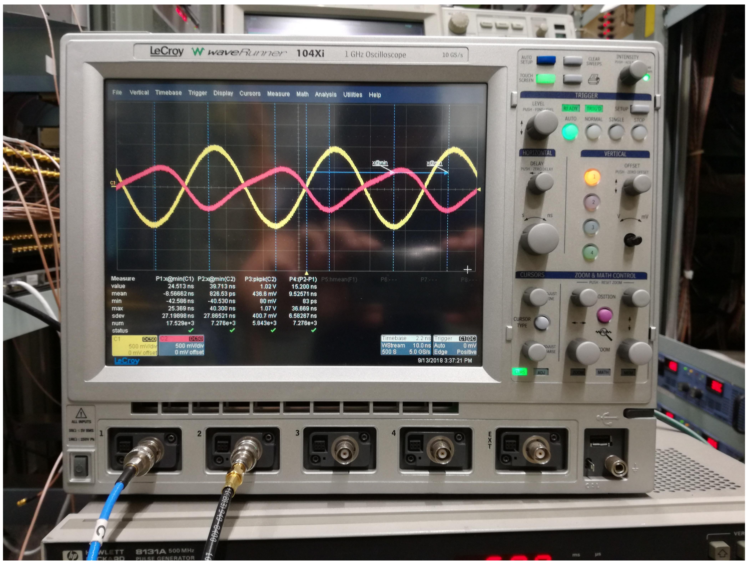

Figure 3.4: Photo of the phase shift measurement: the yellow wave is the reference oscillation, the red one is the signal processed by the system

It was decided to investigate the dependence of the phase shift from the output power: for this reason, some sets of measurements were performed varying also the attenuation. The data collected are shown in Figure 3.5.

It can be noted that the dependence from the attenuation (power) is quite negligible for low powers, while the curve relative to an output power of 30 W slightly deviates from the others. Since the system will probably operate with an output power between 15 W and 30 W, for what concerns the fitting function it was decided to weight differently the various measurements. In particular, the 30 W points were weighted 5 times higher than the other ones, and the obtained fit is shown in red in Figure 3.5. The fact that the phase shift is a relative quantity allowed to translate vertically all of the points in order to get a nice $0° \div 135°$ range.

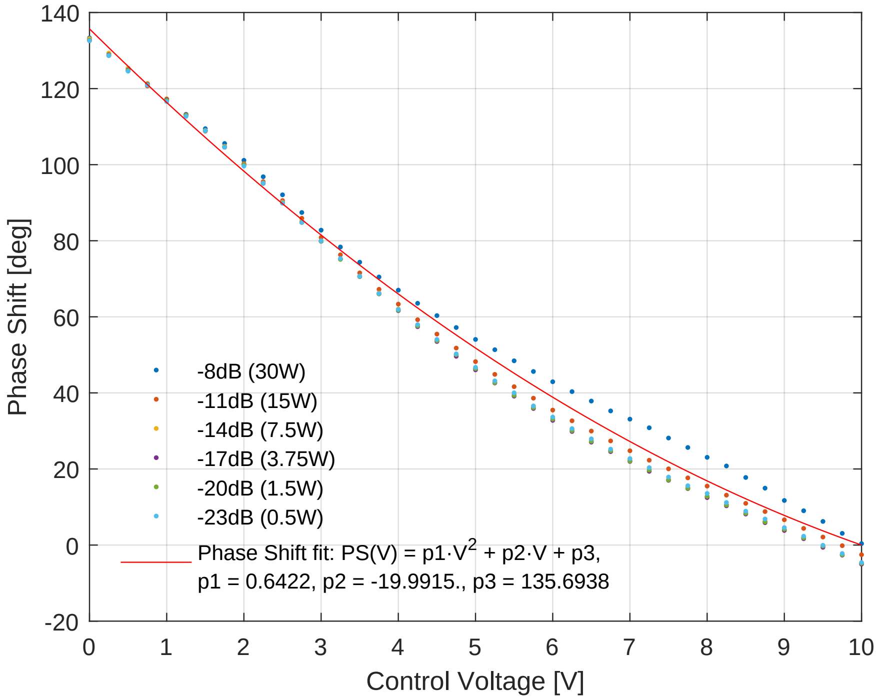

Figure 3.5: Results of the phase shift calibration fitting

Chapter 4

RF Cavity Repair

During the first installation phase of the RF cavity inside IOTA, the ceramic gap of the electron side was broken, leading to the impossibility to obtain vacuum inside the beampipe. This forced to extract the cavity from IOTA ring and to find a strategy to repair the leaking pipe.

First of all the top cover was removed, the cavity beampipe was extracted and the heating system needed for baking of the vacuum was disassembled.

A 3D-printed enclosure was designed to protect the good remaining ceramic gap (the one supposed to work in the protons side) during the mechanical operations connected with the repair.

Since it was impossible to reconnect the damaged ceramic break, it was decided to cut it off and to flip the beampipe section in order to use for the electrons the functioning ceramic gap previously intended for the bunching of protons. In fact, during electron circulation in IOTA the protons side is not energized and therefore there is no need for a ceramic break in that side.

A solid piece of beampipe was welded on each end, substituting the broken ceramic gap. It was decided also to mount one bellow at each end of the pipe, in order to provide it with some mechanical stress relief, while maintaining the possibility to reach a good vacuum.

Of course this is a temporary solution, and for the experiments with protons it will be probably needed to acquire a new beampipe insert with the appropriate ceramic breaks.

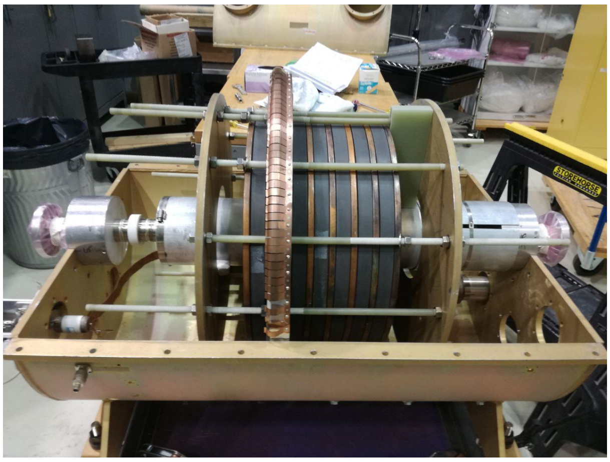

(a)

(b)

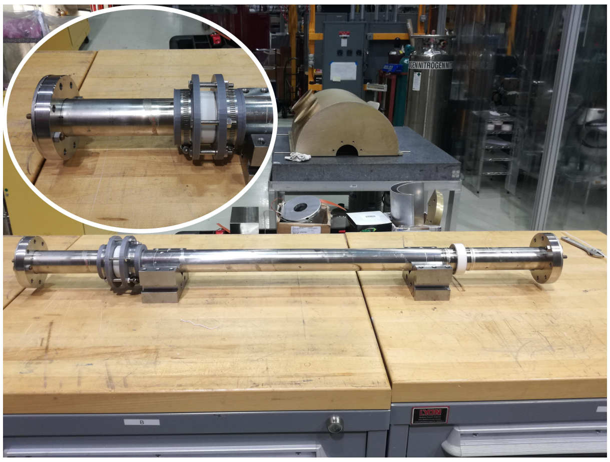

(c)

(d)

Figure 4.1: Successive steps of RF cavity repair: **(a)** the top cover was removed, on the left the broken ceramic gap is visible as a white section in the beampipe, **(b)** the pipe was removed from the cavity and the heating system disassembled, **(c)** on the exposed beampipe, a 3D-printed protection was applied to the functioning ceramic break before the cutting and welding of the broken side **(d)** the welded pipe with new bellows and flanges is leak-checked inside a clean room.

Chapter 5

Conclusions

During the two months of Summer Program the following steps of the low level RF and timing for IOTA ring project have been performed:

- The phase and amplitude controller subsystem has been assembled and quickly characterized on the bench
- The controller was mounted in place, connected to the rest of the system and the software was developed, both on the PLC and on the ACNET side
- A thorough calibration of the attenuator and the phase shifter was performed, and this allowed to derive the parameters for the conversion functions inside the PLC
- The repair of the RF cavity beampipe after the break of a ceramic gap was performed

Future developments of the project include the installation of the repaired RF cavity inside IOTA and the commissioning of the entire RF system with the cavity in place and then also with the beam circulating. The next steps, in a farther perspective, can be the design of a printed circuit board integrating all the RF components, and of course the development of the protons section.

In conclusion, I would like to thank all the people I had the honor and pleasure of working with for this unforgettable experience, first of all my supervisors Kermit Carlson, Dean (Chip) Edstrom and Alexander Valishev. This experience has given me the opportunity to learn a lot about particle accelerators technology, RF and "hands on" electronics, and PLC programming.

Bibliography

[1] AD/APC FAST Facility website. https://fast.fnal.gov/.

[2] *Proposal for an Accelerator R&D User Facility at Fermilab s Advanced Superconducting Test Accelerator*. October 2013.

[3] Gerrit Bruhaug and Kermit Carlson. *The Design and Construction of a Resonance Control System for the IOTA RF Cavity*. August 12, 2016.

[4] Accelerator Division | Operations Department. *FERMILAB Concepts Rookie Book*. December 3, 2013.

[5] Dean (Chip) Edstrom. *A Primer: Productivity 2000 PLCs at FAST*. March 27, 2018.

[6] Donald A. Edwards and M. J. Syphers. *An introduction to the physics of high energy accelerators*. John Wiley and Sons, 1993.

[7] Giacomo Sala. *RF cavity for the IOTA ring at FAST*. Summer internship at Fermilab 2016 Italian Graduate Student Program.

Appendix A

Scripts for data acquisition

A.1 ACL Script for data acquisition

The following code is an ACL script used to set the attenuator control voltage and read the measurements provided by the LP-100A wattmeter. A scan is performed to cover the range 0 V ÷ 10 V in steps of 0.01 V.

Each ACNET device can be accessed using his name (all uppercase in the code); to access the device for reading the name must be preceeded by "N:", while for writing the prefix is "N_". The suffix ".primary" indicates that the variable corresponding to the device inside the PLC is accessed directly, without performing any conversion. For example, the device "IRFEAT" corresponds to the attenuator controller inside the PLC, and its primary value is its control voltage.

```
# Variable attenuator scan for calibration 09/21/18
# https://www-bd.fnal.gov/issues/wiki/ACL

enable settings

# A new .txt file is created to save the data, the name contains a timestamp
fileName = sprintf("wm_daq_%f.txt",millisecondsNow()/1000)
fileID = openFile( fileName, 'w+')

# Set of variables acquired at each iteration:
titlestring = "Control voltage[V], load power[W], loadLogpower[dBm], SWR, load phase[Deg], load impedance[Ohm], timestamp [ms]"
# Printed both on terminal and inside the file
print titlestring
filePrintf(fileID, titlestring)

voltage = 0
while (voltage <= 10)
  set N_IRFEAT.primary voltage    # the new control voltage is set
  wait/sec 1               # 1 second wait for the system response

```

```
  # LP-100A measurements:
  power = N:IRFEFP.primary         # power fed to the load
  powerlog = N:IRFEDB.primary      # power fed to the load [dBm]
  SWR = N:IRFESW.primary               # Standing Wave Ratio
  phase = N:IRFEPH.primary       # phase between voltage and current
  impedance = N:IRFEZ.primary          # load impedance magnitude
  timestamp = millisecondsNow()/1000   # timestamp

  # Printed both on terminal and inside the file
  print voltage ", " power ", " powerlog ", " SWR ", " phase ", " impedance ", " timestamp
  outstring = sprintf("%f, %f, %f, %f, %f, %f, %f\n", voltage, power, powerlog, SWR, phase, impedance, timestamp)
  filePrintf(fileID, outstring)
  voltage += 0.01
endwhile

closeFile(fileID)
```

A.2 Python script for data acquisition

The following code is a Python script for the acquisition of the readings of the HP 437B wattmeter. The wattmeter is connected to the LAN and sends via telnet 20 power measurements every second, therefore the python script simply connects to the instrument and reads the incoming data. One data is separated from the following with a line feed character ('\n'). Not only the raw data are saved into a file, but also a mean is performed every 20 values and saved to a second output file.

```
#HP 437B wattmeter readings acquisition for calibration 09/21/18

import telnetlib
import time
import numpy as np

# Address and port for connection to the wattmeter through telnet
HOST = "131.225.118.77"
PORT = "1234"

tn = telnetlib.Telnet(HOST,PORT)
tn.open(HOST,PORT)

# Two .txt files are created to save the acquired data, their names contain a timestamp
FILENAME1 = "hp_daq_%f.txt"%(time.time())
f1 = open(FILENAME1,"w+")
FILENAME2 = "%s_mean.txt"%(FILENAME1[0:-4])
f2 = open(FILENAME2,"w+")

```

```
print "Press Ctrl+C to interrupt"
i = 0
power = [0] * 20
times = [0] * 20
try:
  while True:
    output = tn.read_until("\n")  # A new line is read from the wattmeter
    timestamp = time.time()     # The timestamp is acquired
    f1.write("%s\t%f\n"%(output[0:-2], timestamp))    # Raw data is saved in file 1
    power[i] = float(output[0:-2])
    times[i] = timestamp
    i = i + 1
    if i == 20:   # The mean of 20 successive acquisitions is saved in file 2
      i = 0
      f2.write("%f\t%f\n"%(np.mean(power), np.mean(times)))
      print np.mean(power), '\t', np.mean(times)
except KeyboardInterrupt:
  pass
tn.close()
f1.close()
f2.close()
```